Available online at www.sciencedirect.com
ScienceDirect
Catalysis Today 124 (2007) 36–42
CATALYSIS TODAY
www.elsevier.com/locate/cattod

Investigation of co-hosted basic and metal nanoparticles in Pt/Cs-BEA zeolites

C. Bisio [a,1], K. Fajerwerg [b], G. Martra [a], P. Massiani [b,*]

[a] *Dipartimento di Chimica IFM & NIS Center of Excellence, Università degli Studi di Torino, via P. Giuria 7, 10125 Torino, Italy*
[b] *Laboratoire de Réactivité de Surface, UMR 7609 du CNRS, Université Pierre et Marie Curie, 4 Place Jussieu, Casier 178, 75252 Paris Cedex 05, France*

Available online 26 March 2007

Abstract

Various acido-basic BEA zeolites having different Cs contents and containing supported Pt particles were prepared using two acidic parent BEA supports with same framework Al content but with strongly different morphology of the zeolite crystallites. In spite of highly different exchange capacities in aqueous solution, the two parent BEA supports behaved similarly towards formation of Cs-oxide like nanospecies. Thus, the addition of a similar amount of Cs was necessary in the two samples to extinguish all Brønsted acidic sites and a further introduction of Cs led to the presence of highly dispersed Cs_2O like species with strong basic character as shown by the adsorption of CO_2 followed at 293 K by FT-IR spectroscopy. FT-IR experiments were also conducted at 100 K and 293 K using CO as probe molecule to give further insights on the Cs and reduced Pt species, respectively. In the presence of co-hosted Cs-oxide like, highly dispersed Pt^0 nanoparticles are formed with sizes close to 1 nm as observed by TEM. Both the high dispersion of the Pt^0 nanoparticles in the more basic samples and the phenomenon of electro-donation by the basic support contribute to the changes in electronic behaviour of the Pt^0 particles shown by FT-IR of adsorbed CO.

Keywords: Basicity; BEA zeolite; Caesium; Platinum; Nanoparticles

1. Introduction

In the field of metal supported heterogeneous catalysts, one advantage of zeolites among classical aluminosilicate supports is to have a high specific area with strongly organized microporous channel systems in which both a high dispersion and a regular distribution of metal nanoparticles can be obtained. Another interest of these supports is the possibility to tune their acid–base properties by simply changing their chemical composition, by both exchange of the countercations and/or occlusion in the microporosity of other phases (e.g., sulfides, oxides), thus possibly modifying the characteristics of the dispersed metal particles through metal–support interaction effects. This is exemplified in this work in which increasing amounts of caesium, in the form of both Cs^+ exchanged ions and Cs-oxide like nanospecies, were introduced into the porosity of two Pt-containing BEA zeolites with the aim to vary their basic properties [1]. The use of FT-IR spectroscopy in the presence of adsorbed CO and CO_2, complemented by TEM and N_2 physisorption experiments, allows us to characterize both the state and location of caesium and to show how the particle size and the electronic properties of dispersed platinum vary when the basicity of the Cs-containing BEA support increases.

2. Experimental

2.1. Materials

The two parent acidic BEA zeolites, henceforth abbreviated as H-BEA_{ENI} (Si/Al = 13) and H-BEA_{RIPP} (Si/Al = 16), were provided by Polimeri Europa S.P.A (Italy) and the Research Institute for Petroleum Processing (China), respectively. As illustrated elsewhere [2], these two samples exhibit X-ray diffractograms typical of the BEA structure with, however, slightly less intense and broader diffraction peaks in the case of H-BEA_{ENI} that is made of very small nanocrystallites with a

* Corresponding author.
E-mail address: massiani@ccr.jussieu.fr (P. Massiani).
[1] Present address: Dipartimento di Scienze e Tecnologia Avanzate, Università del Piemonte Orientale "A. Avogadro", via Bellini 25/G, 15100 Alessandria, Italy.

0920-5861/$ – see front matter © 2007 Elsevier B.V. All rights reserved.
doi:10.1016/j.cattod.2007.02.009

mean size of *ca*. 80 nm, whereas the crystallites in H-BEA$_{RIPP}$ are quite regular in shape and sizes (between 200 and 500 nm), as shown by SEM. Related to these textures, the microporous volume is slightly smaller in H-BEA$_{ENI}$ than in H-BEA$_{RIPP}$ (0.20 and 0.25 mL g^{-1}, respectively).

Before their use, both samples were calcined at 823 K in flowing air to ensure full template removal and surface cleaning. Then, they were ion exchanged at 323 K under stirring for 2 h in a 0.5N aqueous solution of CsCl (100 mL g^{-1} zeolite); the procedure was repeated three times using each time a fresh CsCl solution and the Cs-exchanged solids were washed in deionized water. Next, platinum was added by preparing a stirred aqueous suspension containing the zeolite (100 mL g^{-1} of zeolite) and adding dropwise a given volume of a 2.5×10^{-2} M [Pt(NH$_3$)$_4$Cl$_2$] solution calculated as to introduce a nominal content of about 1.0 wt% of Pt in the zeolite (weight of Pt per weight of TO$_2$ (T = Si or Al) framework in the suspension, in %). After exchange, the sample was thoroughly washed in deionized water and then dried overnight in an oven at 80 °C. In order to increase further the Cs contents, parts of the above Pt containing samples were submitted to an incipient wetness impregnation with a CsOH solution containing 0.6 Cs atom per Al atom in the zeolite. Before characterizations, the exchanged (Pt/Cs-BEA$_{RIPP}$ and Pt/Cs-BEA$_{ENI}$) and impregnated (Pt/Cs*-BEA$_{RIPP}$ and Pt/Cs*-BEA$_{ENI}$) samples were calcined at 723 K for 2 h in order to decompose the NH$_3$ ligands of the parent Pt tetraammine complex. A low heating rate (50 K h^{-1}) and a high air flow (800 mL min^{-1}) were used in order to prevent any autoreduction process [3].

2.2. Methods

Chemical compositions (contents of Cs, Al, Si and Pt) were measured by inductively coupled plasma atomic emission spectroscopy (ICP-AES) in the Central Analysis Service of the CNRS (France).

FT-IR measurements were performed on a Bruker IFS66 spectrometer (resolution 4 cm^{-1}). The self-supported wafers (*ca*. 15 mg of sample pressed at 5 tonnes cm^{-2}) were placed into a conventional IR cell equipped with KBr windows. Before adsorption of CO at 100 K (20 Torr, 1 Torr = 133.33 Pa) and of CO$_2$ at r.t. (100 Torr), the samples were previously dehydrated *in situ* for 3.5 h at 673 K (4 K min^{-1}) under dynamic vacuum (residual pressure $<10^{-5}$ Torr). The adsorption of CO at r.t. (30 Torr) was performed after *in situ* reduction of the samples in the FT-IR cell performed by, firstly, dehydrating the sample for 5 h at 773 K (5 K min^{-1}) in dynamic vacuum, then, admitting 100 Torr of H$_2$ into the IR cell and keeping it in contact with the sample for 5 h. The reduced wafer was finally evacuated for 1 h at 773 K and cooled down to room temperature under dynamic vacuum. All gases employed were high-purity grade and were used without further purification.

Porosities were characterized by N$_2$ physisorption on a Micromeritics ASAP 2010 instrument. The adsorption–desorption isotherms were registered at 77 K after preliminary evacuation of the samples at 573 K under vacuum. The microporous volumes were determined using the *t*-plot method. They were normalized per g of zeolite TO$_2$ framework (where T = Si or Al), *i.e.* by considering solely the mass of dehydrated Si$_x$Al$_y$O$_2$ support but not that of heavy Cs, the content of which changes from one sample to another.

Transmission electron microscopy (TEM) was used to evaluate the size and distribution of the Pt particles after reduction performed *ex situ* in flowing H$_2$ (50 mL min^{-1}) at 773 K (5 K min^{-1}) for 4 h. The micrographs were registered on a JEOL 2010 instrument (200 kV) equipped with a LaB$_6$ filament. In order to ensure presence of the Pt particles in the core of the zeolitic grains, the observations were made on samples previously embedded in an epoxy resin and cut in microtome slices thinner than 60 nm. The histograms of metal particle sizes were established by considering at least 1000 particles and the data were used to evaluate an average diameter of the particles as $d = \sum n_i d_i / \sum n_i$, where n_i is the number of particles with d_i diameter.

3. Results and discussion

3.1. Chemical contents and remaining acidity

Table 1 reports the chemical contents of the four samples, expressed as atomic ratios and Pt wt%. As indicated in Section 2.1, both the H-BEA$_{ENI}$ and H-BEA$_{RIPP}$ zeolites have close Al contents, as it is still the case after the exchange and impregnation treatments, the samples of the BEA$_{ENI}$ series being only slightly richer in Al (Si/Al $\approx$ 12.6) than those of the BEA$_{RIPP}$ series (Si/Al $\approx$ 16.5). Also, the Pt content is similar in all samples, close to 1 wt%, which indicates that all the metal ions of the Pt(NH$_3$)$_4$Cl$_2$ solution were introduced into the zeolite during the exchange procedure.

Besides these similarities, a main difference takes place with respect to the Cs contents after exchange in solution. Thus, in Pt/Cs-BEA$_{ENI}$, the atomic Cs/Al ratio is only 55% of that obtained in Pt/Cs-BEA$_{RIPP}$. Furthermore, if considering the ratio (Cs + 2Pt)/Al, *i.e.* the overall countercations/Al ratio that takes into account the fact that two Cs$^+$ cations were removed from the solid for each (divalent) tetraammine platinum complex introduced during the step of exchange in the Pt(NH$_3$)$_4$Cl$_2$ solution, it is seen that the exchange was completed in Pt/Cs-BEA$_{RIPP}$ (ratio equal to 0.96) whereas the ratio remains as low as 0.56 for Pt/Cs-BEA$_{ENI}$, confirming the low exchange capacity of this sample.

Low exchange levels in zeolites are often related to the presence of a significant amount of extra-framework Al atoms that do not generate any framework negative charge. In a previous paper reporting FT-IR data of adsorbed NH$_3$ [4], we showed that H-BEA$_{ENI}$ contains a low amount of extra-framework Al with Lewis acid character, and we demonstrated that the lack of about 40% of the exchange capacity in aqueous solution of this zeolite is rather due to a process of reversible opening of part of the framework Si–O–Al bonds when this sample with nanosized zeolite crystallites is put in presence of water. Upon dehydration, both the tetrahedral framework environments and their ''associated'' protons were recovered, and we could demonstrate that the content in protons

Table 1
Codes and chemical compositions of the samples of the BEA_{ENI} and BEA_{RIPP} series.

Sample name	Method of Cs addition[a]	Chemical compositions				Remaining acidity[c]	Average Pt^0 particle size[d] (Å)
		Atomic ratios			Pt[b] (wt%)		
		Cs/Al	Si/Al	Pt/Al			
$Pt/Cs\text{-}BEA_{ENI}$	Exch.	0.46	12.6	0.050	1.20	0.44	18
$Pt/Cs^*\text{-}BEA_{ENI}$	Exch. + Imp.	1.08	12.7	0.047	1.11	0	12
$Pt/Cs\text{-}BEA_{RIPP}$	Exch.	0.83	16.3	0.059	1.10	0.05	16
$Pt/Cs^*\text{-}BEA_{RIPP}$	Exch. + Imp.	1.61	16.7	0.061	1.13	0	11

[a] Cs introduced by exchange in solution only (Exch.) or by exchange in solution and additional impregnation (Exch. + Imp.).
[b] Weight percentage of Pt (±0.1) per gram of dehydrated TO_2 (T = Si or Al) zeolite framework.
[c] Calculated from chemical analysis as the atomic (Al–Cs–2Pt)/Al ratios.
[d] Measured from TEM micrographs as the $\sum n_i d_i / \sum n_i$ ratios, where n_i is the number of particles with d_i diameter.

(remaining Brønsted acidity) well fitted with the number of sites that were not exchanged in solution, such a number being possibly expressed as (Al–Cs–2Pt)/Al ratio that considers all expected cationic sites minus those exchanged by Cs^+ and $Pt(NH_3)_4^{2+}$ ions in solution. Such ratios are reported in Table 1 for all present samples, thus informing on their remaining Brøntsed acidity, still important in $Pt/Cs\text{-}BEA_{ENI}$. On the contrary, all Brønsted acid sites are suppressed in the impregnated $Pt/Cs^*\text{-}BEA_{ENI}$ and $Pt/Cs^*\text{-}BEA_{RIPP}$ samples containing a small (Cs/Al = 1.08) and higher (Cs/Al = 1.61) Cs overloading, respectively.

3.2. Basic properties

Having identified different acidic properties for the above samples, we characterized their related basic behaviours by conducting a FT-IR study of the adsorption of CO_2 that is known to form various types of carbonates when interacting with basic centers [4,5], thus producing characteristic IR bands in the 1800–1350 cm^{-1} domain.

After admission of CO_2, a weak but well-defined band is visible at *ca.* 1380 cm^{-1} for all samples (Fig. 1), fully reversible upon evacuation ($<10^{-5}$ Torr, spectra not shown). As reported in the literature, this component is due to the in phase stretching mode of CO_2 molecules weakly adsorbed on cationic sites. Actually, the resulting slight polarization of the adsorbed CO_2 renders partly IR active such a vibrational mode. A much intense band due to the IR active out of phase stretching mode of CO_2 adsorbed on cations was observed around 2350 cm^{-1} (not shown) [4,7]. In addition, for both exchanged $Pt/Cs\text{-}BEA_{ENI}$ (Fig. 1a) and $Pt/Cs\text{-}BEA_{RIPP}$ (Fig. 1c) with no Cs overloading, a weak component in the 1750–1550 cm^{-1} range is observed, slightly more intense and centered at 1630 cm^{-1} in the case of $Pt/Cs\text{-}BEA_{RIPP}$ that contains more Cs. This component is attributable to monodentate carbonate-like species formed by fixation of CO_2 on framework oxygen atoms rendered basic enough by the proximity of Cs^+ countercations [4–11]. Their number should increase as the number of Cs^+ ions increases, which is indeed in line with our observation. Also, the intensity of the bands increases slightly with contact time and remain rather small even after 35 min of contact with CO_2 (Fig. 1a′ and c′), indicating a progressive and limited formation of such carbonates, in line with the rather weakly basic character of zeolitic framework oxygen centers [1].

In contrast, upon contact of CO_2 with both impregnated $Pt/Cs^*\text{-}BEA_{ENI}$ (Fig. 1b) and $Pt/Cs^*\text{-}BEA_{RIPP}$ (Fig. 1d), an intense band centered at *ca.* 1670 and a pair of bands at *ca.* 1340 and 1314 cm^{-1} are immediately visible. These bands can be straightforwardly assigned to bidentate carbonates (likely at least two species) issued from the reaction of CO_2 with basic Cs_2O like particles [12] formed upon calcination of Cs-enriched samples [13,14]. In line with this attribution, the band intensities are the highest for the Cs-richest $Pt/Cs^*\text{-}BEA_{RIPP}$ sample (Fig. 1d–d′). Besides, several observations can be drawn from the spectra. Firstly, in the case of $Pt/Cs^*\text{-}BEA_{RIPP}$, the maximum band intensity is almost reached after immediate contact of CO_2 with the sample (compare Fig. 1d and d′), which reveals a rapid formation of carbonates and therefore a high basic strength of the related Cs-oxide like centers. Secondly, the

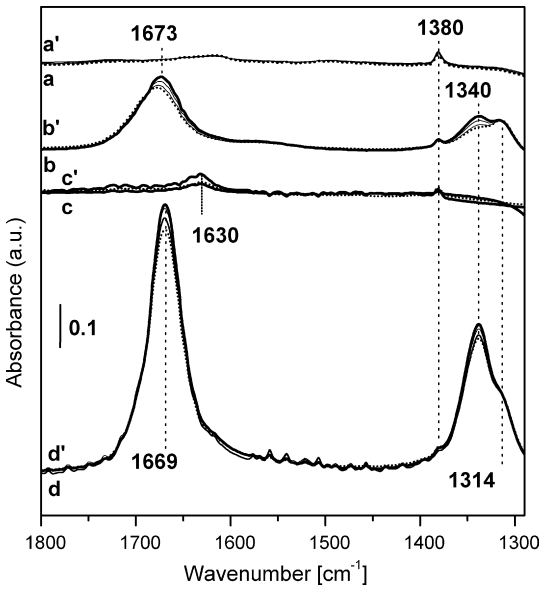

Fig. 1. FT-IR spectra after admission of 100 Torr of CO_2 at 293 K on: (a–a′) $Pt/Cs\text{-}BEA_{ENI}$, (b–b′) $Pt/Cs^*\text{-}BEA_{ENI}$, (c–c′) $Pt/Cs\text{-}BEA_{RIPP}$ and (d–d′) $Pt/Cs^*\text{-}BEA_{RIPP}$; spectra (a–d) immediately after admission then upon progressive increase of contact (intermediate spectra) and finally (a′–d′) after 35 min. All spectra are reported after subtraction of the corresponding spectrum before CO_2 adsorption.

formation of carbonates is more progressive on Cs-poorer Pt/Cs*-BEA_{ENI} (compare Fig. 1b and b′), revealing a lower average basicity in this sample for which, moreover, a progressive shift from 1678 to 1673 cm^{-1} and a regular increase of the band at 1340 cm^{-1} suggest the presence of sites of different basic strengths. Thirdly, the high band intensities, particularly in the case Pt/Cs*-BEA_{RIPP}, indicate that such strongly basic sites are numerous, suggesting that the Cs-oxide species formed upon calcination of the Cs-overloaded samples are present as nanoparticles, highly dispersed all over the zeolite microporosity. The high dispersion of such Cs-based nanoparticles and their oxidic nature were also confirmed by, respectively, combined TEM/EDX experiments and EXAFS data, as reported elsewhere [4].

3.3. Occupancy of the zeolite micopores by Cs^+ cations and Cs_2O nanoparticles

Beside the chemical effect commented on above, the replacement of protons by bulkier Cs^+ countercations (0.169 nm) and the dispersion in the zeolite channels of Cs_2O like nanoparticles resulted, also, in the change of a physical feature of the samples, namely the microporous void space that decreased progressively as more and more Cs was introduced. For both BEA_{ENI} and BEA_{RIPP} series, the loss of microporosity with increasing Cs content took place in a comparable manner (Fig. 2), indicating a similar steric effect of Cs whatever the parent zeolite, and therefore a comparable state of dispersion inside the porosity.

Additional findings on the consequence of introducing Cs into the BEA micropores were provided by the FT-IR spectra of CO adsorbed at low temperature. In view of the Cs contents that are 10–30 times higher than that of Pt in all samples, the FT-IR signals can be interpreted mainly in terms of adsorption of CO on the Cs Lewis centers. Consquently, we neglected in the discussion below the very weak contribution of carbonyls of cationic platinum that will be detailed in a next paper.

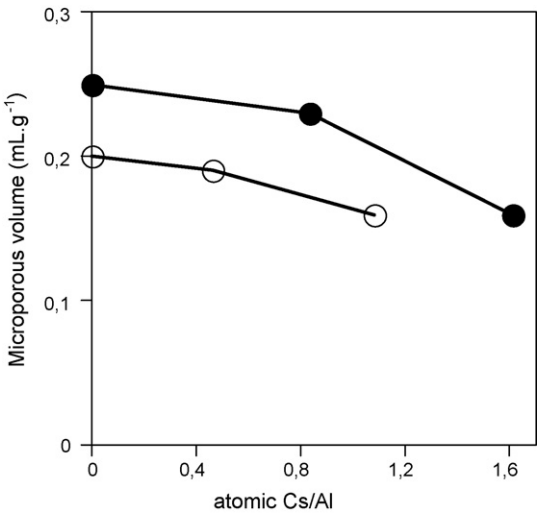

Fig. 2. Evolution of the microporous volume as a function of the Cs/Al ratio in the BEA_{ENI} (open symbols) and BEA_{RIPP} (full symbols) series of samples.

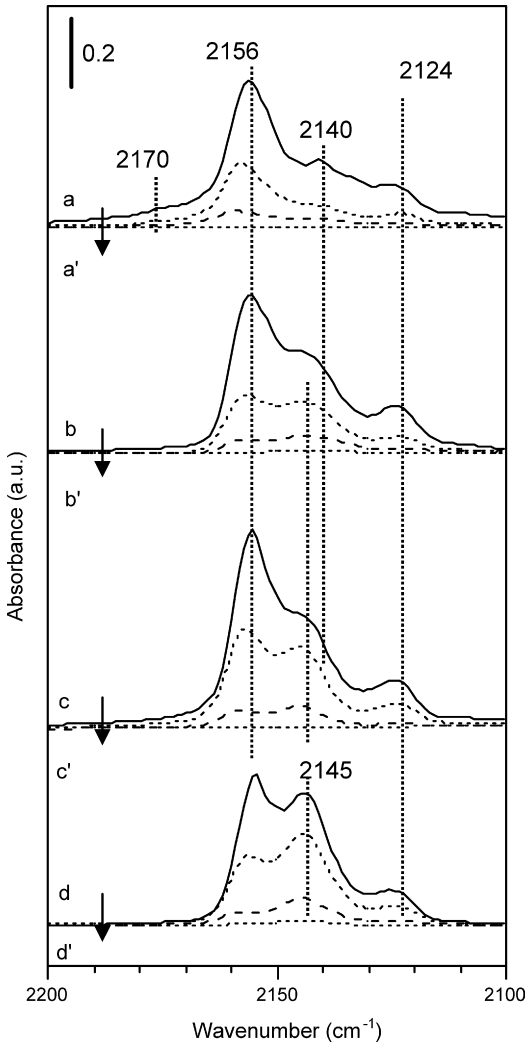

Fig. 3. FT-IR spectra after admission of 20 Torr of CO at 100 K on: (a–a′) Pt/Cs-BEA_{ENI}, (b–b′) Pt/Cs*-BEA_{ENI}, (c–c′) Pt/Cs-RIPP and (d–d′) Pt/Cs*-RIPP; spectra (a–d) immediately after admission, then during progressive evacuation (intermediate spectra) until reaching (a′–d′) 10^{-4} Torr. All spectra are reported after subtraction of the corresponding spectrum before CO adsorption.

In the case of Pt/Cs-BEA_{ENI} (Fig. 3a), the spectrum exhibited various bands easily assignable from literature. Firstly, the main peak at 2156 cm^{-1} and its partner band at 2124 cm^{-1} are indicative of CO adsorbed on Cs^+ Lewis acid centers through the C-end [15–18] and O-end [19–24], respectively. These two components decreased in a parallel mode when diminishing the CO coverage (Fig. 3a–a′), confirming their common origin. Secondly, the component at 2140 cm^{-1} is related to liquid-like CO condensed within the pores [25]. Finally, the weak signal identified at 2170 cm^{-1} is typical of CO interacting with protons, still partially present in this sample, as reported above (see Section 3.1 and Table 1). All these components decreased in intensity until full disappearance upon outgassing (Fig. 3a–a′). The band at 2140 cm^{-1}, related to CO stabilised in the weakest way in the pores, *i.e.* in the liquid-like form, was the first to be depleted.

As expected, the adsorption of CO on Pt/Cs-BEA_{RIPP} also led to the pair of bands of CO adsorbed on Cs^+ Lewis centers

(2156 and 2124 cm^{-1}) but the signal of CO adsorbed on protons was no longer present, in line with the almost complete H^+/Cs^+ exchange in this sample. Besides, the most peculiar feature of the spectra was constituted by a broad and quite intense component at *ca*. 2145 cm^{-1} that, on its low frequency side, likely contains the contribution at 2140 cm^{-1} of liquid like CO. Among the various signals, the 2145 cm^{-1} component exhibited the higher resistance to outgassing although it finally disappeared as occurred for the others (Fig. 3c–c′).

As for the assignment of the 2145 cm^{-1} band, the combination of (i) its position, at a frequency which is lower than that of CO adsorbed via C-end on single Cs^+, (ii) the higher resistance to CO outgassing, which indicates adsorption on sites with a higher polarizing power and (iii) the absence of a component related to partner CO species adsorbed through the O-end, allows to propose that it is due to CO anchored both by the carbon and oxygen atoms to two cations. Such a head–tail Cs^+–CO–Cs^+ interaction with a pair of cations is known to lower the stretching frequency [15,26,27] and it would justify the somewhat higher stability. Bands with similar behaviours were already reported for CO adsorbed on halides [26,27], in oxides [28] or in zeolites [29]. Interestingly, a structural information could be derived from this spectroscopic feature, as the head–tail adsorption of CO between two Cs^+ requires two cations located not too far, suggesting a consequent local ‘‘crowding’’ of countercations in some part of the zeolite channels. However, more work involving modelling approaches would be needed before getting precise insights on such Cs^+–CO–Cs^+ configurations in the BEA channels.

For CO adsorbed on both Cs-overloaded Pt/Cs*-BEA_{ENI} (Fig. 3b–b′) and Pt/Cs*-BEA_{RIPP} (Fig. 3d–d′), the spectral patterns were essentially the same as above, an important point being the absence of any new band that could have been attributed specifically to CO interacting with Cs^+ ions at the surface of the Cs_2O like nanoparticles dispersed in the pores. Therefore, it has to be assumed that the Lewis acidity of such Cs^+ surface centers is quite similar to that of Cs^+ countercations, making the FT-IR technique in presence of adsorbed CO unable to discriminate between these different types of Cs^+ ions. Then, the band at 2145 cm^{-1} should concern all CO molecules stabilised between two Cs^+ ions in a head–tail form, these ions being present either as countercations, incorporated at the surface of basic oxide nanoparticles or being a mixture of both. Noteworthy, this band is already present for Pt-BEA_{ENI} with low excess of Cs (Pt/Cs*-BEA_{ENI}) and it is particularly intense for Cs-richest Pt/Cs*-BEA_{RIPP} (Fig. 3d–d′), confirming again the high dispersion of overloaded caesium in the BEA microporosity.

3.4. Effect of co-hosted caesium on Pt metal particles

Both series of samples were finally investigated after reduction in H_2, with the aim to obtain information on the size and surface states of the Pt metal particles, using the techniques of TEM and FT-IR spectroscopy of adsorbed CO, respectively.

As for the size of the Pt particles, Fig. 4 displays for Pt/Cs-BEA_{ENI} taken as a representative example, a typical TEM micrograph showing reduced Pt^0 particles (dark spots) homogeneously distributed within the zeolite grains (images taken on microtomic slices). Such homogeneous distributions were found for all samples, except that for Pt/Cs-BEA_{RIPP} few Pt particles larger than 30 nm, located on the external surface of the zeolite crystallites, were also present.

From the observation of all micrographs, the Pt particles appeared significantly smaller in size in the case of both Pt/Cs*-BEA_{ENI} and Pt/Cs*-BEA_{RIPP} with excess of Cs, suggesting a higher Pt dispersion in these Cs-enriched zeolites. This was better quantified by making a statistical evaluation of the Pt particle size distributions (more than 1000 particules counted for each sample) and plotting the histograms of particle sizes as illustrated for Pt/Cs-BEA_{ENI} (Fig. 4a) and Pt/Cs*-BEA_{RIPP} (Fig. 4b) that are the two extremes of the series of materials in

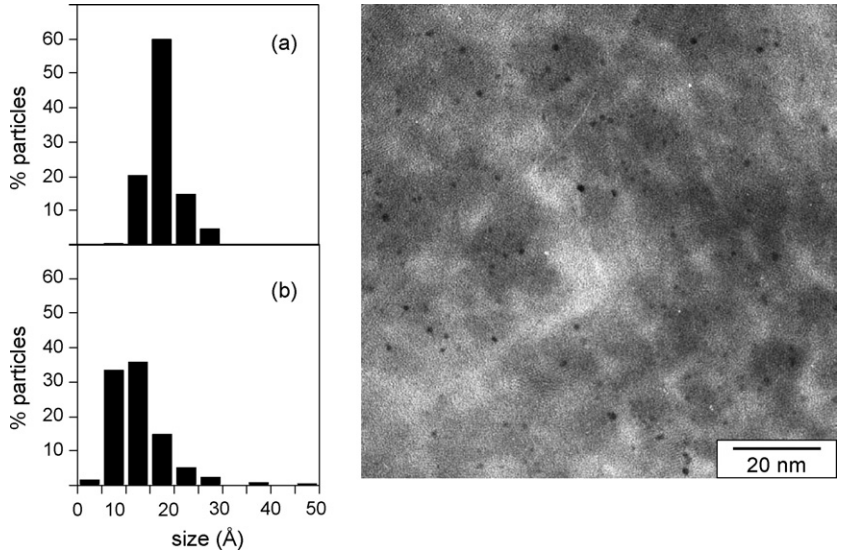

Fig. 4. Transmission electron micrograph of a microtomic slice of reduced Pt/Cs-BEA_{ENI}, and histograms of the Pt^0 particle sizes in: (a) Pt/Cs-BEA_{ENI} and (b) Pt/Cs*-BEA_{RIPP}.

terms of Cs content. The values of the average Pt particle sizes obtained from these measurements are reported in Table 1. In both Cs-overloaded Pt/Cs*-BEA_{ENI} and Pt/Cs*-BEA_{RIPP}, the average Pt particle size is close to 1 nm, significantly smaller than the value of 1.6–1.8 nm obtained for the solely exchanged Pt/Cs-BEA_{ENI} and Pt/Cs-BEA_{RIPP} samples. Thus, the Pt dispersion is enhanced when co-hosted Cs-oxide like nanoparticles are present. It can be assumed that the increased occupancy of the channels by the bulky Cs^+ countercations and Cs_2O like nanoparticles, as indicated above by volumetric and IR measurements, plays a role in decreasing the ''mean free path'' of Pt atoms and cluster along the channels during the reducing treatment, decreasing the possibility of their aggregation. An additional reason could be a change in the nature and reducibility of the calcined Pt species present before reduction when the co-hosted basic phase is present or not, as already suggested from TPR data [2,30].

Finally, a peculiar effect of the co-hosting of Pt and Cs_2O like nanoparticles was probed by studying the metal surface states by FT-IR spectroscopy of CO adsorbed at 293 K, *i.e.* at a temperature at which CO is adsorbed solely on the Pt particles, its interaction with the Cs^+ sites being then too weak to take place. The admission of CO on reduced Pt/Cs-BEA_{ENI} (Fig. 5a) produced a well shaped band at 2085 cm^{-1}, hereafter referred to as high frequency (HF) band, located in a range classically reported for CO linearly adsorbed on supported Pt metal particles of few nanometers in size [31]. This band is accompanied by a weak and broad component centred at *ca.* 1850 cm^{-1}, hereafter referred to as low frequency (LF) band, due to CO adsorbed in a bridged form [31]. In the case of Pt/Cs-BEA_{RIPP}, both bands appeared less intense and downshifted, the HF one being located at 2075 cm^{-1} and broadened towards the low frequency side (Fig. 5c). The lower intensity should hardly be due to the above-mentioned presence of quite large Pt particles on the external surface of the zeolite grains (see Section 2.2), since such particles should exhibit a low specific surface area and then poorly contribute to the spectrum. Therefore, the observed band can be ascribed to small particles

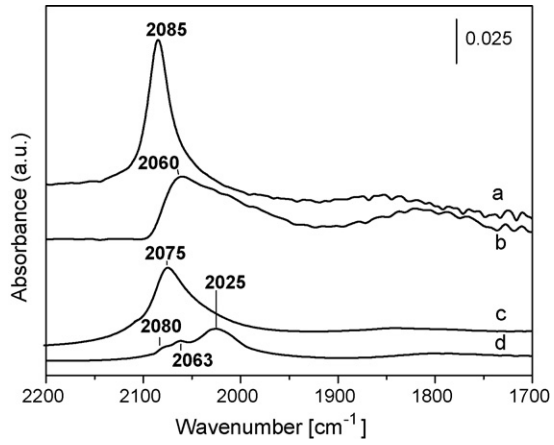

Fig. 5. FT-IR spectra after 1 min of admission of 30 Torr of CO at 293 K on reduced: (a) Pt/Cs-BEA_{ENI}, (b) Pt/Cs*-BEA_{ENI}, (c) Pt/Cs-BEA_{RIPP} and (d) Pt/Cs*-BEA_{RIPP}. All spectra are reported after subtraction of the corresponding spectrum before CO adsorption.

in the pores of the zeolites, and both the observed downshift in position (HF and LF) and the broadening (HF) appear characteristic of the combination of a decrease in particle size and an interaction with more basic framework oxygen atoms as the H^+/Cs^+ exchange almost reaches completion.

However, more significant differences were observed in the case of the samples containing Cs_2O like particles. As for Pt/Cs*-BEA_{ENI} (Fig. 5b), the HF band exhibits a maximum at 2060 cm^{-1}, with a series of unresolved sub-bands of decreasing intensity spreading down to 1960 cm^{-1}, while the LF component appears increased in intensity and downshifted to *ca.* 1820 cm^{-1}. Such spectral changes should result from a significantly increased availability of electron charge for back donation from the Pt metal to adsorbed CO probe molecule, that in turns should derive from an enrichment in electron density of the Pt particles by interaction with the support. Such effects were already described in the case of metal interacting with basic zeolites [32,33] or with strong basic oxides [34] as the Cs_2O-like nanoparticles should be (as indicated by the adsorption of CO_2, see Section 3.2). Also, changes of the main exposed surface sites due to the diminishing of the particle sizes could play a role [35,36]. Passing now to the Pt/Cs*-BEA_{RIPP} sample (Fig. 5d), both bands appear significantly decreased in intensity but the HF band is no longer spread on a so wide range as before, exhibiting a maximum at 2025 cm^{-1} and a partly resolved component at 2063 cm^{-1}, and the maximum of the LF band is located at *ca.* 1790 cm^{-1}. Such changes in position wetness for a further increase of the interaction of the Pt particles with the basic co-hosted phase, more abundant in this sample. Noteworthy, the weak spectral intensity, actually the lowest in the overall series of spectra, unexpected on the basis of the size of Pt nanoparticles, suggests that the Cs-oxide like phase might cover part of the co-hosted Pt metal particles.

4. Conclusion

The chemical and FT-IR study of two series of Pt-containing Cs^+-exchanged BEA samples with comparable framework Si/Al but different sizes of the zeolite crystallites shows that the level of cationic exchange of BEA in solution may strongly depend on the textural characteristics of the sample. In the case of the parent H-BEA zeolite appearing in the form of very small nanocrystallites with a mean size of *ca.* 80 nm, the exchange capacity in solution is solely *ca.* 60% of that expected from the framework Al content. This limitation is due to the presence of *ca.* 40% of framework Si–O–Al bonds reversibly breakable by water. Consequently, CsOH impregnation followed by calcination is necessary in this nanosized sample to complete the exchange of all available protons and to form a Cs-oxide like nanophase with strong basic strength dispersed in the micropores as attested by the formation of a significant amount of carbonates upon adsorption of CO_2 followed by FT-IR spectroscopy. Starting from the parent BEA sample with bigger crystallites, the exchange capacity in solution is straightforwardly related to the Al content, as usually expected for zeolites, and the Cs overloading introduced by CsOH

impregnation is all converted to a Cs-oxide like phase upon calcination, leading to a higher amount of dispersed Cs_2O like nanoparticles and to enhanced basic properties. The progressive Cs enrichment in the BEA porosity also leads to a typical evolution of the FT-IR signals in the presence of CO, with progressive appearance of a new band at 2145 cm^{-1} assigned to a Cs^+–CO–Cs^+ head–tail configuration, that does not permit however, to discriminate between Cs^+ cations present either as countercations or at the surface of the Cs-oxide like species. In the two series of BEA samples, the presence of the strongly basic Cs-based phase modifies the properties of co-hosted platinum. Thus, the metal dispersion is enhanced and Pt nanoparticles with sizes of the order of 1 nm or below are formed. Both the decrease of the sizes of the Pt particles and their possible interaction with the neighbor co-hosted Cs_2O like phase with strong basic properties induce an electronic enrichment at the surface of the metal particles.

Acknowledgments

The CNRS, the French–Italian Universities and Compagnia di San Paolo (supporting NIS) are gratefully thanked for fundings. P. Beaunier from ''Service Commun of Electron Microscopy'' in UPMC and J.M. Krafft from LRS are acknowledged for their contributions to TEM and FT-IR analyses, respectively. L. Stievano is gratefully thanked for the preparation of samples.

References

[1] D. Barthomeuf, Catal. Rev. Sci. Eng. 38 (1996) 521.
[2] L. Stievano, P. Massiani, C. Caldeira, M.F. Ribeiro, Stud. Surf. Sci. Catal. 142A (2002) 359.
[3] P. Gallezot, Catal. Rev. Sci. Eng. 20 (1979) 121.
[4] C. Bisio, P. Massiani, K. Fajerwerg, L. Sordelli, L. Stievano, E.R. Silva, S. Coluccia, G. Martra, Micropor. Mesopor. Mater. 90 (2006) 175.
[5] G. Busca, V. Lorenzelli, Mater. Chem. 7 (1982) 89.
[6] J.C. Lavalley, Catal. Today 27 (1996) 377.
[7] B. Bonelli, B. Civalleri, B. Fubini, P. Ugliengo, C. Otero Area'n, E. Garrone, J. Phys. Chem. B 104 (2000) 10978.
[8] L. Bertsch, H.W. Habgood, J. Phys. Chem. 67 (1963) 1621.
[9] P.A. Jacobs, F.M. van Cauwelaert, E.F. Vansant, J. Chem. Soc., Faraday Trans. I 69 (1973) 2130.
[10] M. Forster, M. Schumann, J. Chem. Soc., Faraday Trans. I 85 (1989) 1149.
[11] J.W. Ward, H.W. Habgood, J. Phys. Chem. 70 (1966) 1178.
[12] S. Huber, Dissertation, Ludwig-Maximiliams-Universitat Munich, 1997.
[13] P.E. Hathaway, M.E. Davis, J. Catal. 116 (1989) 279.
[14] M. Lasperas, H. Cambon, D. Brunel, I. Rodriguez, P. Geneste, Micropor. Mater. 7 (2–3) (1996) 61.
[15] N.S. Hush, M.L. Williams, J. Mol. Spectrosc. 50 (1974) 349.
[16] A. Zecchina, E. Escalona Platero, C. Otero Areán, J. Catal. 107 (1987) 244.
[17] P. Ugliengo, U.P. Saunders, E. Garrone, J. Phys. Chem. 93 (1989) 2117.
[18] K.I. Hadjiivanov, G.N. Vayssilov, Adv. Catal. 47 (2002) 307.
[19] V. Bosácek, D. Freude, Stud. Surf. Sci. Catal. 37 (1988) 231.
[20] V. Gruver, J. Fripiat, J. Phys. Chem. 98 (1994) 8549.
[21] A. Zecchina, S. Bordiga, C. Lamberti, G. Spoto, L. Carnelli, C. Otero Arean, J. Phys. Chem. 98 (1994) 9577.
[22] A. Sheete, V. Kamble, N. Gupta, V. Kartha, J. Phys. Chem. B 102 (1998) 5581.
[23] V. Kamble, N. Gupta, V. Kartha, R. Iyer, J. Chem. Soc., Faraday Trans. 89 (1993) 1143.
[24] A.M. Ferrari, K.M. Neymann, N. Rösch, J. Phys. Chem. B 101 (1997) 9292.
[25] V. Gruver, A. Panov, J.J. Fripiat, Langmuir 12 (1996) 2505.
[26] D. Scarano, A. Zecchina, J. Chem. Soc., Faraday Trans. 1 (82) (1986) 3611.
[27] S. Coluccia, Stud. Surf. Sci. Catal. 48 (1989) 289.
[28] S. Coluccia, M. Baricco, L. Marchese, G. Martra, A. Zecchina, Spectrochim. Acta A 49 (1993) 1289.
[29] S. Bordiga, G. Turnes Palomino, C. Pazé, A. Zecchina, Micropor. Mesopor. Mater. 34 (2000) 67.
[30] C. Bisio, C. Caldeira, V. Dal Santo, G. Martra, P. Massiani, R. Psaro, M.F. Ribeiro, J.M. Silva, L. Stievano, Inorg. Chim. Acta 349 (2003) 227.
[31] N. Sheppard, T.T. Nguyen, in: R.J.H. Clark, R.E. Hester (Eds.), Advances in Infrared and Raman Spectroscopies, vol. 5, Heyden & Son Ltd., 1978, pp. 67–149.
[32] T. Becue, F.J. Maldonado-Hodar, A.P. Antunes, J.M. Silva, M.F. Ribeiro, P. Massiani, M. Kermarec, J. Catal. 181 (1999) 244.
[33] L. Sordelli, G. Martra, R. Psaro, C. Dossi, S. Coluccia, Top. Catal. 8 (1999) 237.
[34] M. Primet, J.M. Basset, M.V. Mathieu, M. Prettre, J. Catal. 29 (1973) 213.
[35] M.J. Kappers, J.T. Miller, D.C. Koningsberger, J. Phys. Chem. 100 (1996) 3227.
[36] G. Blyholder, J. Phys. Chem. 68 (1964) 2772.